

# Burst Lost Probabilities in a Network with Simultaneous Link Possession: A Single-Node Decomposition Approach

Tzvetelina Battestilli  
MCNC Grid Computing and Network Services  
Advanced Technology Group  
Research Triangle Park, NC 27709 USA  
lina@mcnc.org

Harry Perros  
Computer Science Department  
North Carolina State University  
Raleigh, NC 27695 USA  
hp@csc.ncsu.edu

Stefanka Chukova  
School of Mathematics, Statistics and Computer Science  
Victoria University  
Wellington, New Zealand  
stefanka@mcs.vuw.ac.nz

July 21, 2006

## Abstract

We present a novel analytical method of evaluating the performance of Optical Burst Switched (OBS) Networks. We consider OBS networks where the size of the data bursts varies and the link distance between two adjacent network elements also varies depending on the network's topology. This leads to the *simultaneous link possession problem*, where a burst dynamically acquires and reserves wavelengths for only a portion of its source-destination route but not the entire route. Our solution to this problem has two parts. First, we develop a queueing network model that accurately portrays the simultaneous link possession scenario. Next, we develop a fast single-node decomposition algorithm to compute the burst loss probabilities in the network. Our algorithm extends the link-decomposition method from teletraffic theory by allowing the dynamic simultaneous link possession. We use simulation to validate the high accuracy of our algorithm.

## 1 Introduction

The backbone of the next generation Internet will most likely be an optical network because of the unprecedented data rates and low bit error rates that can be achieved with optics and fibers. Today, most of the wavelength division multiplexed (WDM) optical networks of the Internet, operate over point-to-point links, where optical-to-electrical-to-optical conversion is required at each network node. Future WDM designs envision a hybrid optical network where the data plane remains end-to-end in the optical domain while the control and management planes are in the optical domain during transmission and

in the electrical domain for processing. The switching architectures of these future optical networks can be classified into circuit switched (OCS), packet switched (OPS) and burst switched (OBS). In a circuit switched network, long-term circuit connections (lightpaths), are setup between the source and destination nodes. In an OPS network the user traffic is carried in optical packets along with the in-band control information. The control info is extracted and electronically processed at each node. The successful operation of an OPS network requires the availability of practical optical buffers and practical optical header processing. Unfortunately, both of these technologies are years away.

Given the current state of the optical technology, the Optical Burst Switched (OBS) network is a feasible near-term solution. The name optical burst switching comes from the fact that the data is transported in variable size units, called *bursts*. Due to the great variability of the duration of a burst, they can be viewed as lying between optical packet switched and circuit switched networks. That is, when all bursts durations are very short, equal to the duration of an optical packet, then the OBS network can be seen as resembling an OPS network. On the other hand, when all burst durations are extremely long, then the OBS network can be seen as resembling a circuit switched optical network. The OBS idea combines the best features of circuit switching and packet switching [1]. Its dynamic nature allows for network adaptability and scalability, which makes it very suitable for the transmission of Internet traffic.

The term OBS is used to describe a variety of architectures and protocols [2]. However, OBS does have some definitive common characteristics. Most importantly, in OBS the data and the corresponding control information are transmitted separately in time and space through the network. The data in OBS comes from upper layer traffic which could be IP, SONET, ATM, Frame Relay, GbEthernet, etc. An OBS end-device collects this upper-layer traffic, sorts it per OBS destination address and assembles it into variable size *bursts* [3]. For each burst, the OBS end-device constructs a *control packet*, which is transmitted an *offset* time prior to the transmission of the burst. As the control packet travels along the route, it is electronically processed and it reserves bandwidth resources for its corresponding burst. Upon receipt of the control packet, an OBS node schedules a free wavelength on the desired output port and configures its switching fabric to transparently switch the upcoming burst. The burst itself travels transparently as an optical signal from the source to the destination. This is advantageous because the OBS nodes just switch the optical signals without knowing the format or the transmission rate of the burst data.

In order to decrease the *end-to-end* transmission delay, most OBS architectures use a one-way signaling scheme. The transmitting end-devices do *not* wait for a positive acknowledgment from the destination end-devices that the control packet has been successful at reserving resources at each hop along the route. Instead, they wait the *offset* time and then transmit the burst. Therefore a burst may be dropped if it arrives at an OBS node, where the control packet was unsuccessful at reserving a wavelength on its desired output port. In view of this, the calculation of the burst loss probability is an important measure of the performance of an OBS network.

The performance of the various OBS protocols [3, 1, 4] has been studied both through simulation and analytical models. The analytical studies mostly focus on a single output port of an OBS node and assume Poisson arrivals and full wavelength conversion [5, 6, 7]. Since these studies assume no buffers, the OBS output port is modeled as an M/G/W loss system, where W is the number of wavelengths, and the Erlang-B formula is used to calculate the burst loss probability. There are also studies of OBS with fiber delay lines [8, 6] or deflection routing [9, 10]. OBS with quality of service (QoS) classes has

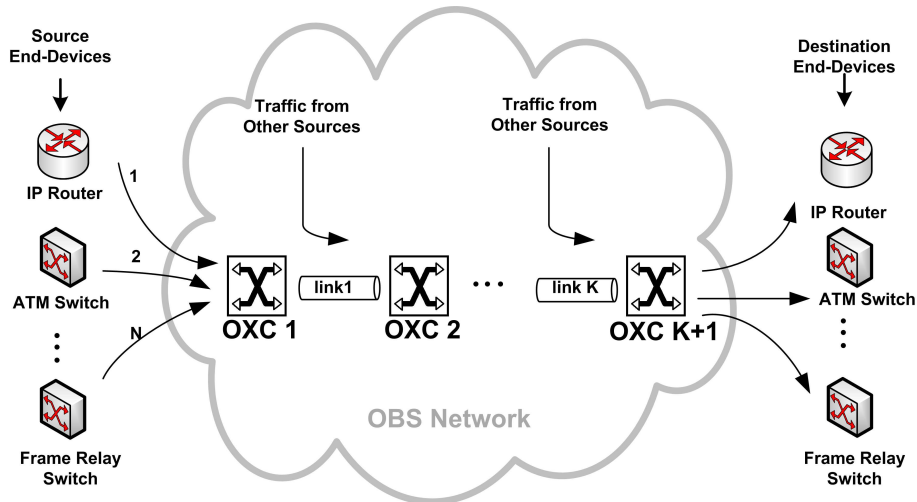


Figure 1: A Path in an OBS Network

been investigated in [11, 6, 12] and an OBS architecture with centralized-signaling and guaranteed QoS classes is proposed in [13].

All of the previously cited analytical models focus on a single OBS node. These models provide a limited insight about the overall performance of an OBS network. An analytical model of an OBS network is proposed in [14, 15], where the OBS network is modeled by a network of loss nodes, each representing a link of  $W$  wavelengths. Bursts are assumed to arrive in a Poisson fashion and each burst occupies a single wavelength on each link along its source-destination path until it is lost or until it departs from the network.

The focus of this paper is the end-to-end performance of an OBS network, where the bursts *dynamically* acquire and release wavelengths from link to link as they travel from their source to their destination and it is organized as follows. In Section 3 we describe the network under study and the proposed queueing network model. Next, in Section 4 we propose a novel algorithm that solves for the bursts loss probabilities in the network and in Section 5 we give an illustrative example. We validate the accuracy of our analytical method in Section 6 and conclude in Section 7.

## 2 The OBS Network Under Study

We study an OBS network, where the core nodes are made of an Optical Crossconnects (OXC) and an electronic control unit. Two adjacent OXCs are linked by a single WDM link (fiber), which has  $W + 1$  transmission wavelengths. The first  $W$  wavelengths are used for burst transmission while the  $(W + 1)^{st}$  wavelength is used to transmit control information. Each OBS node has a full wavelength conversion capability, i.e., in the case of contention at an output port it can optically convert an optical signal from one wavelength to another. Also, there are no fiber delay lines (FDL) buffers available at the network nodes and thus a burst is lost if it arrives at an output port where all the wavelengths are busy.

We analyze the performance of a specific source-destination transmission path, made of  $K$  links.

Therefore, we consider  $(K + 1)$  OXCs connected in tandem, as shown in Figure 1, where the traffic flows only from left to right. A number of transmitting OBS end-devices, linked to OXC 1, transmit bursts to a number of OBS end-devices, linked to OXC  $(K + 1)$ . Each transmitting OBS end-device is linked to OXC 1 by a single fiber and it may be equipped with one or more transmitters. We refer to the traffic generated from the transmitting end-devices as the *main traffic*. In addition, to the main traffic we consider traffic generated by any other sources in the OBS network. This traffic arrives at the intermediate links of the considered path. We refer to this traffic as the *cross burst traffic*.

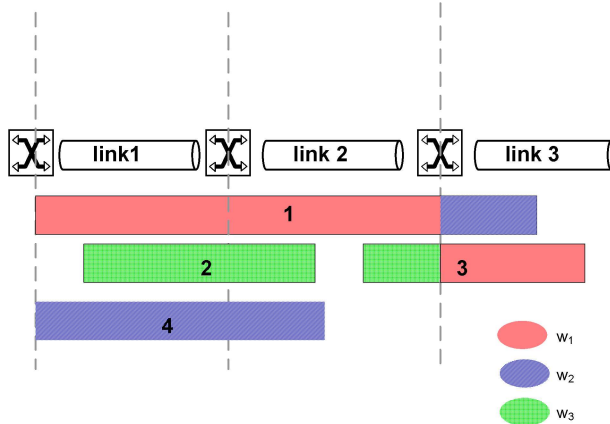


Figure 2: Bursts simultaneously hold wavelengths on multiple links

Each burst holds simultaneously wavelengths on one or more links, but not all of the links, along its source-destination path. We call this phenomenon *dynamic simultaneous link possession* and we illustrate it in Figure 2. Depending on the size of a burst and the link lengths between OXCs, a burst may hold wavelengths on one, two, three or even more links. Due to the full wavelength conversion capability at each OBS node, a burst may occupy one wavelength on one link and the same or different wavelength on the next link. A burst frees up the wavelength on a link as soon as its tail departs the OXC. Also, we assume that as soon as the head of a burst enters a link then its assigned wavelength will be occupied for the duration of the burst transmission. For example, in Figure 2, burst 1 holds simultaneously wavelengths on three links,  $w_1$  on links 1 and link 2 and  $w_2$  on link 3, burst 2 holds wavelength  $w_3$  on link 2, burst 3 occupies only the wavelength  $w_1$  on link 3 and burst 4 possesses wavelength  $w_2$  on link 1 and link 2.

### 3 The Queuing Network Model

We propose the queuing network model in Figure 3 for an OBS path of  $K$  links, where the bursts simultaneously hold wavelengths on consecutive links. Since there is no buffering, in our queuing model there are *no* queues and burst loss is possible at each node. Each queuing node has  $W$  servers, where  $W$  is the number of data wavelengths per link. Each node in the queuing network does not represent the state of a physical link but rather, as explained below, it represents the number of bursts that occupy wavelengths on a certain number of successive links.

The queuing network from Figure 3 is viewed in separate rows, where each row represents the transmission of bursts with a specific size. For example, the top row of the queuing network models the

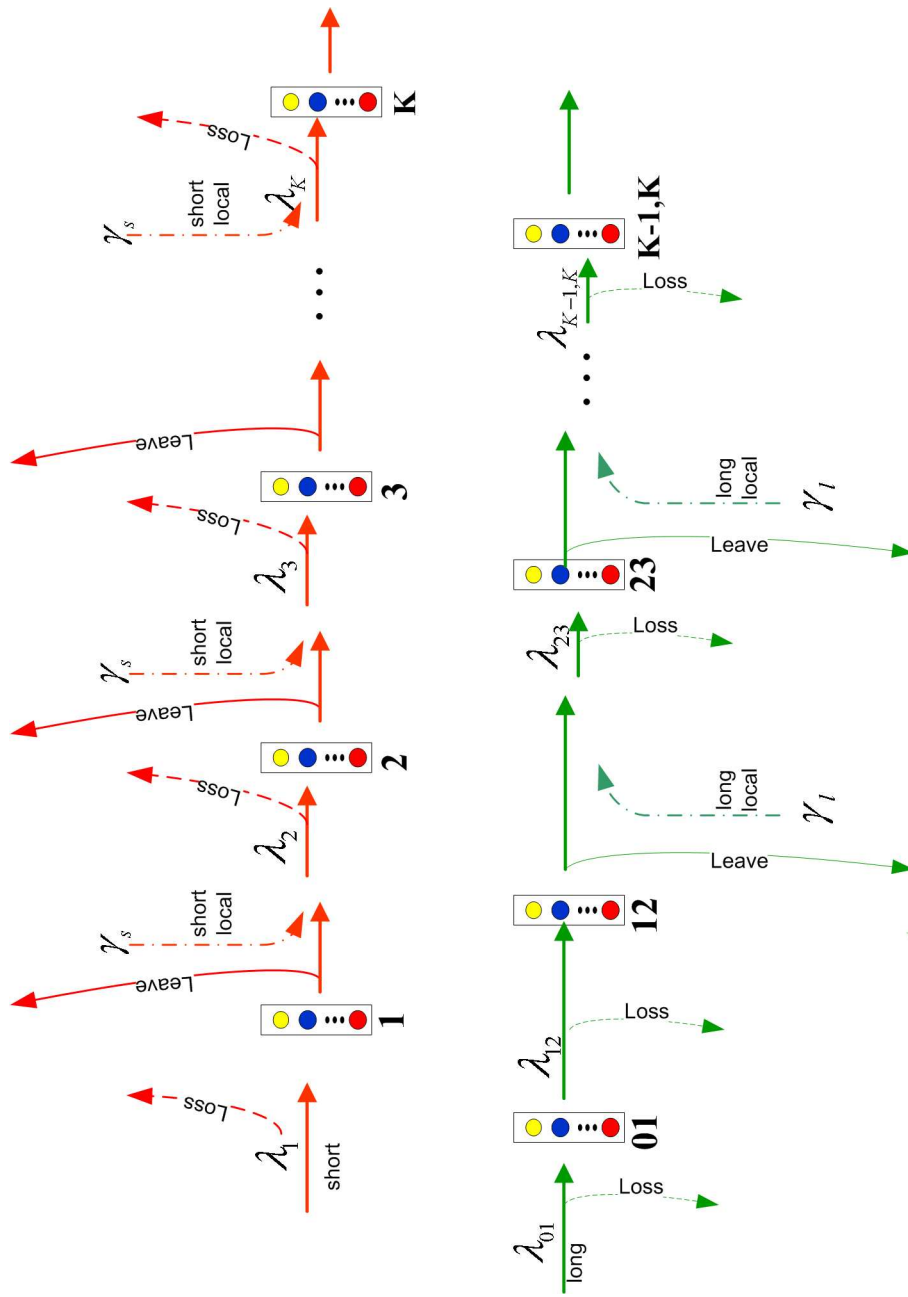


Figure 3: Queueing Model for an OBS Network with Simultaneous Link Possession

transmission of bursts that occupy a wavelength on only one link as they travel along the OBS path. These bursts propagate by moving from one loss node of the top row to the next. Node  $i$ ,  $1 \leq i \leq K$ , represents the number of bursts currently holding a wavelength on link  $i$ . The second row of the queueing network models the transmission of bursts that hold wavelengths on two consecutive links as they travel the OBS path. These bursts move strictly along the nodes of the second row. Node 01 represents the bursts being transmitted from the end-device through OXC 1 and link 1 and thus only occupying a wavelength on link 1. Upon exiting node 01 this burst moves to node 12, where it simultaneously occupies a wavelength on link 1 and a wavelength on link 2. Node  $(i, i + 1)$ ,  $1 \leq i \leq K - 1$ , represents the number of bursts simultaneously holding wavelengths on link  $i$  and link  $(i + 1)$ . Due to the full wavelength conversion capability at each OBS node, these bursts may occupy one wavelength on link  $i$  and the same or different wavelength on link  $(i + 1)$ .

For simplicity, in Figure 3 we have only shown the queueing network for two different burst sizes: bursts that occupy wavelengths on one link and bursts that occupy wavelengths on two consecutive links. If in the OBS network there are bursts with larger size, i.e., bursts that occupy wavelengths on three consecutive links, then there would be an additional third row added to the description of the queueing network. In the third row each loss node will model three consecutive links of the OBS path. This idea can be extended to bursts that span any number of links.

The main traffic, as defined in Section 2, is assumed to be Poisson-distributed and its average arrival rate at link 1 is  $\lambda_1$  for the short bursts and  $\lambda_{01}$  for the long bursts. The cross burst traffic is also Poisson-distributed and its average rate is  $\gamma_s$  for the short bursts and  $\gamma_l$  for the long bursts. A burst holds a wavelength on a link for an exponential amount of time with mean  $1/\mu$ . The cross traffic intersects the path and it may depart at any of the intermediate links. We denote the *intermediate* arrival rates of short bursts at node  $i$  by  $\lambda_i$ ,  $1 \leq i \leq K$  and the arrival rates of long bursts at node  $(i, i + 1)$  by  $\lambda_{i,i+1}$ ,  $0 \leq i \leq K - 1$ .

## 4 Analysis of the Model: Solving for the burst loss probabilities

In steady state, the queueing network, described in Section 3, does not have a product form solution that can be used to obtain the burst loss probabilities. Therefore, we developed a single-node decomposition algorithm, where each node is solved individually while taking into account the constraints that arise from the simultaneous link possession. The algorithm begins by obtaining an initial guess for the burst loss probabilities by assuming independence between the nodes of the queueing network, i.e., ignoring the simultaneous link possession. Using the initial guess the queueing network is solved again by taking into account the fact that each physical link of the OBS path is modeled by three nodes of the queueing network. We do this by solving related the M/M/W loss system with *modified* arrival rates based on probability information from adjacent nodes. This is done for both short and long nodes iteratively. We outline the details of the algorithm below but first we introduce the following notations:

- $\pi_i(j)$  ( or  $\pi_{i,i+1}(j)$  ): steady state probability that there are  $j$  bursts at node  $i$  ( or node  $(i, i + 1)$  )
- $M_i$  ( or  $M_{i,i+1}$  ): main traffic (or main) burst loss probability at node  $i$  ( or node  $(i, i + 1)$  )
- $C_i$  ( or  $C_{i,i+1}$  ): cross traffic (or cross) burst loss probability at node  $i$  ( or node  $(i, i + 1)$  )

- $P_i^k(j)$ : *Prob* {link  $i$  is not full |  $n_k = j$ }, i.e., the conditional probability that the wavelengths of the physical link  $i$  are not all busy, given that there are  $j$  bursts at queueing node  $k$ . Node  $k$  is one of the three queueing nodes that model link  $i$ : node  $n_{i-1,i}$ , node  $n_i$  and node  $n_{i,i+1}$ . At a short node,  $k = i$  and thus,  $P_i^i(j) = \text{Prob} \{n_{i-1,i} + n_{i,i+1} < (W - j) | n_i = j\}$ . At a long node,  $k = (i - 1, i)$  or  $k = (i, i + 1)$  and thus,  
 $P_i^{i-1,i}(j) = \text{Prob} \{n_i + n_{i,i+1} < (W - j) | n_{i-1,i} = j\}$  or  
 $P_i^{i,i+1}(j) = \text{Prob} \{n_{i-1,i} + n_i < (W - j) | n_{i,i+1} = j\}$  respectively.
- $I_i$  ( or  $I_{i,i+1}$ ): indicator of cross burst arrivals at node  $i$  ( or node  $(i, i + 1)$  ). It is equal to 1 if cross burst arrivals are present and it is equal to 0 otherwise.

## 4.1 Initial Guess

The burst loss probabilities are initialized by solving for the steady state of each queueing node independently from the other nodes in the queueing network, i.e., ignoring the simultaneous link possession. Thus, in order to obtain the steady state probabilities for each node, we solve corresponding the M/M/W loss system [16]. Therefore, for the short nodes we obtain

$$\pi_i(j) = \pi_i(0) \prod_{m=0}^{j-1} \frac{\lambda_i}{(m+1)\mu}, \quad 0 \leq j \leq W, 1 \leq i \leq K \quad (1)$$

and for the long nodes

$$\pi_{i,i+1}(j) = \pi_{i,i+1}(0) \prod_{m=0}^{j-1} \frac{\lambda_{i,i+1}}{(m+1)\mu}, \quad 0 \leq j \leq W, 0 \leq i \leq K - 1, \quad (2)$$

where  $\pi_i(0)$  and  $\pi_{i,i+1}(0)$  are found using the probability normalizing condition. Note that  $\pi_i(W)$  is the Erlang's B formula, which is usually denoted by  $B(W, \lambda_i/\mu)$  and it represents the percentage of time (or the probability) that all wavelengths are busy. Similarly,  $\pi_{i,i+1}(W) = B(W, \lambda_{i,i+1}/\mu)$ .

The intermediate arrival rates  $\lambda_i$ ,  $2 \leq i \leq K$  and  $\lambda_{i,i+1}$ ,  $1 \leq i \leq K - 1$  are approximated by a Poisson process and are calculated based on the carried load from the previous node. This approximation is valid only if the burst loss probabilities are very small, which is expected in a well-designed OBS network.

In the initial guess, the blocking probabilities for the bursts are approximated by the Erlang-B relation, i.e., for the short bursts, allowing for the presence of cross traffic, we have

$$M_i = B(W, \lambda_i/\mu) \quad \text{and} \quad (3)$$

$$C_i = I_i B(W, \lambda_i/\mu). \quad (4)$$

Analogously, for the long bursts we obtain

$$M_{i,i+1} = B(W, \lambda_{i,i+1}/\mu) \quad \text{and} \quad (5)$$

$$C_{i,i+1} = I_{i,i+1} B(W, \lambda_{i,i+1}/\mu). \quad (6)$$

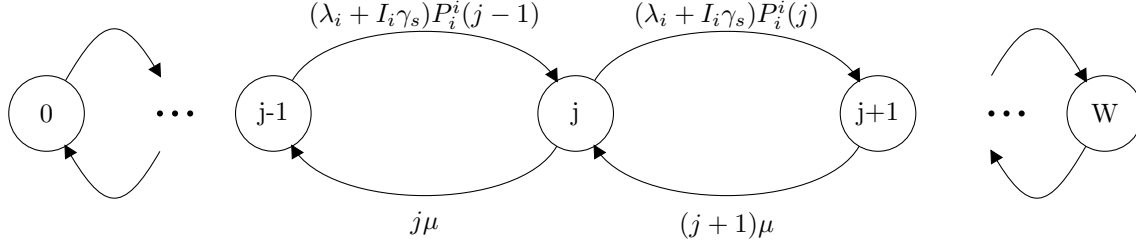


Figure 4: State Transition Modified Rate Diagram for Short Nodes

## 4.2 Analysis of the Short Nodes

Next we carry out the analysis of the short nodes. The arrival rate to a short node  $i$  is the carried traffic from the previous short node (see Figure 3), i.e.,

$$\lambda_i = (\lambda_{i-1})(1 - M_{i-1}) + I_{i-1}\gamma_s(1 - C_{i-1}), \quad 2 \leq i \leq K. \quad (7)$$

For a short node  $i$  the state transition modified rate diagram is shown in Figure 4. The state of this diagram  $j$ ,  $0 \leq j \leq W$ , represents the number of short bursts  $n_i$  that currently occupy a wavelength on link  $i$ . The arrival rates are modified based on the availability of a wavelength on the link  $i$  at the burst arrival. This availability is calculated using probability information from the adjacent nodes because each physical link is modeled by three queueing nodes. So for short node  $i$ , a burst requires a wavelength on link  $i$ , which is also modeled by the long nodes  $(i-1, i)$  and  $(i, i+1)$ . Therefore the conditional probability that there is a free wavelength on link  $i$  given that  $n_i = j$  depends on the steady state probability vectors of the long nodes  $(i-1, i)$  and  $(i, i+1)$ . Thus

$$\begin{aligned} P_i^i(j) &= \text{Prob} \{ \text{link } i \text{ not full} \mid n_i = j \}, \quad 1 \leq j \leq W, 1 \leq i \leq K \\ &= \text{Prob} \{ n_{(i-1,i)} + n_{(i,i+1)} < (W - j) \mid n_i = j \} \\ &= \sum_{s=0}^{W-j} \pi_{i-1,i}(s) \sum_{t=0}^{W-j-s} \pi_{i,i+1}(t) \end{aligned} \quad (8)$$

We write the cross balance equations for the transition rate diagram from Figure 4 and derive the steady state probabilities to be

$$\pi_i(j) = \pi_i(0) \frac{(\lambda_i + I_i \gamma_s)^j}{j! \mu^j} \prod_{m=0}^{j-1} P_i^i(m) \quad 1 \leq j \leq W, 1 \leq i \leq K, \quad (9)$$

where  $\pi_i(0)$  is found using the probability normalizing condition.

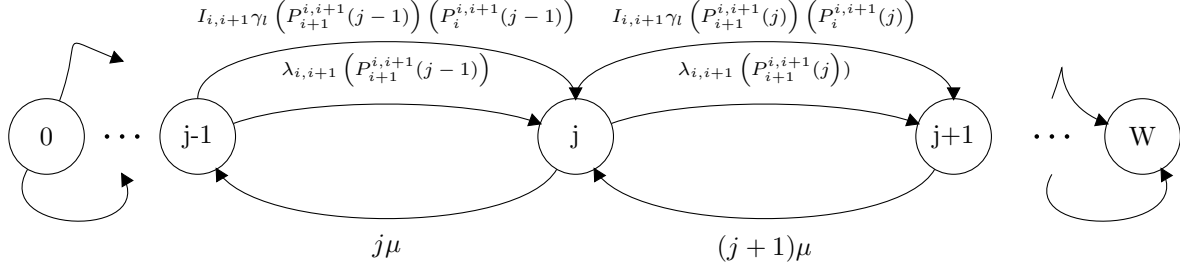


Figure 5: State Transition Modified Rate Diagram for Long Bursts

Next, we calculate the blocking probabilities for the main traffic and the cross traffic at a short node. These two probabilities are equal because a short burst only needs to obtain a wavelength on link  $i$ . Therefore, the main blocking probability is

$$\begin{aligned}
M_i &= \sum_{j=0}^W \pi_i(j) \text{Prob}\{\text{link } i \text{ is full} | n_i = j\}, \quad 1 \leq i \leq K \quad (10) \\
&= \sum_{j=0}^W \pi_i(j) \text{Prob}\{n_{i-1,i} + n_{i,i+1} \geq (W - j) | n_i = j\} \\
&= \sum_{j=0}^W \pi_i(j) (1 - P_i^i(j))
\end{aligned}$$

and the cross blocking probability is

$$C_i = I_i M_i, \quad 1 \leq i \leq K. \quad (11)$$

### 4.3 Analysis of the Long Nodes

In what follows, using a similar approach as in 4.2, we analyse the long nodes. The arrival rate to a long node  $(i, i + 1)$  is the rate of the carried traffic from the previous long node, i.e.,

$$\lambda_{i,i+1} = \lambda_{i-1,i} (1 - M_{i-1,i}) + I_{i-1,i} \gamma_l (1 - C_{i-1,i}), \quad 1 \leq i \leq K - 1. \quad (12)$$

Figure 5 shows the state transition modified rate diagram for a long node  $(i, i + 1)$ . The state  $j$ ,  $0 \leq j \leq W$ , is the number of long bursts  $n_{i,i+1}$  that occupy a wavelength on links  $i$  and  $i + 1$ . As in the case of short burst, the transition rates are modified using probability information on the availability of a free wavelength on the required link, namely:

- main arrivals of long bursts at node  $(i, i + 1)$  require a wavelength only on link  $(i + 1)$  because they already possess a wavelength on link  $i$ . Therefore for the main bursts, we obtain the conditional

probability that physical link  $(i + 1)$  has a free wavelength given that  $n_{i,i+1} = j$ , i.e.,  $P_{i+1}^{i,i+1}(j)$ . As in the case of the short bursts, this conditional probability is calculated based on the fact that each physical link is modeled by three queueing nodes. Link  $(i + 1)$  is modeled by  $n_{i,i+1}$ ,  $n_{i+1}$  and  $n_{i+1,i+2}$ . Therefore,

$$\begin{aligned} P_{i+1}^{i,i+1}(j) &= Prob \{ \text{link } i+1 \text{ is not full} \mid n_{i,i+1} = j \}, \quad 1 \leq j \leq W, 0 \leq i \leq K-1 \quad (13) \\ &= Prob \{ n_{(i+1)} + n_{(i+1,i+2)} < (W - j) \mid n_{i,i+1} = j \} \\ &= \sum_{s=0}^{W-j} \pi_{i+1}(s) \sum_{t=0}^{W-j-s} \pi_{i+1,i+2}(t) \end{aligned}$$

- cross long bursts at node  $(i, i + 1)$  require wavelengths on links  $i$  and  $i + 1$ . Therefore, we need to obtain the conditional probabilities  $P_{i+1}^{i,i+1}(j)$  and  $P_i^{i,i+1}(j)$ . The first probability is found by (13). The second one is the conditional probability that link  $i$  is not full given that  $n_{i,i+1} = j$  and it is obtained similarly.

Based on the transition diagram in Figure 5, we write the cross balance equations and find the steady state probabilities for the long nodes to be

$$\begin{aligned} \pi_{i,i+1}(j) &= \frac{\pi_{i,i+1}(0)}{j! \mu^j} \prod_{m=0}^{j-1} P_{i+1}^{i,i+1}(m) \left( \lambda_{i,i+1} + I_{i,i+1} \gamma_l P_i^{i,i+1}(m) \right), \quad 1 \leq j \leq W, \\ & \quad 0 \leq i \leq K-1, \quad (14) \end{aligned}$$

where  $\pi_{i,i+1}(0)$  is obtained using the probability normalization condition.

For long bursts, the blocking probabilities of the main traffic and the cross traffic differ. This is due to the fact that the main traffic needs to acquire a wavelength on only one link while the cross traffic needs to acquire wavelengths on two links. For the main traffic we obtain that the blocking probability is equal to

$$\begin{aligned} M_{i,i+1} &= \sum_{j=0}^W \pi_{i,i+1}(j) Prob \{ \text{link } i+1 \text{ is full} \mid n_{i,i+1} = j \} \quad (15) \\ &= \sum_{j=0}^W \pi_{i,i+1}(j) Prob \{ n_{i+1} + n_{i+1,i+2} \geq (W - j) \mid n_{i,i+1} = j \} \\ &= \sum_{j=0}^W \pi_{i,i+1}(j) \left( 1 - P_{i+1}^{i,i+1}(j) \right), \quad 0 \leq i \leq K-1, \end{aligned}$$

while the blocking probability for the cross traffic is equal to

$$\begin{aligned} C_{i,i+1} &= I_{i+1} \sum_{j=0}^W \pi_{i,i+1}(j) Prob \{ \text{links } i \text{ or } i+1 \text{ are full} \mid n_{i,i+1} = j \} \quad (16) \\ &= I_{i+1} \sum_{j=0}^W \pi_{i,i+1}(j) \left( 1 - P_i^{i,i+1}(j) \right) \cup \left( 1 - P_{i+1}^{i,i+1}(j) \right), \quad 0 \leq i \leq K-1. \end{aligned}$$

## 4.4 The Single-Node Decomposition Algorithm

If the links in the network consist of a large number of wavelengths, computing the burst loss probabilities becomes quite involved. In order to avoid these difficulties, we propose a Single-Node decomposition algorithm. It solves for the short and the long nodes iteratively until a precespified convergence criterion is satisfied and assure that the iterative values of the burst loss probabilitis converge. In the description of the algorithm, the superscript  $m$  refers to the iteration number. The convergence condition is met when the steady-state probabilities satisfy

**Initial Step,  $m=1$ ;**

**for**  $i = 1 : K$  **do**

//calculate arrival rates based on the carried traffic from previous node ;

**if**  $i = 1$  **then**

$\lambda_i^{(1)}$  and  $\lambda_{01}^{(1)}$  are given;

**else**

$\lambda_i^{(1)}$  use (7) and  $\lambda_{i-1,i}^{(1)}$  use (12);

**end**

//Solve for the steady state probability vectors;

$\pi_i^{(1)}$  use (1) and  $\pi_{i-1,i}^{(1)}$  use (2);

//The blocking probabilities;

$M_i^{(1)} = \pi_i^{(1)}(W)$  and  $C_i^{(1)} = I_i M_i^{(1)}$ ;

$M_{i-1,i}^{(1)} = \pi_{i-1,i}^{(1)}(W)$  and  $C_{i-1,i}^{(1)} = I_{i-1,i} M_{i-1,i}^{(1)}$ ;

**end**

**Iterative Step, start with  $m=2$ ;**

**repeat**

**for**  $i = 1 : K$  **do**

**if**  $i \neq 1$  **then**

$\lambda_i^{(m)}$  use (7) and  $\lambda_{i-1,i}^{(m)}$  use (12);

**end**

//Solve for the steady state probability vectors ;

$\pi_i^{(m)}$  use (9) and  $\pi_{i-1,i}^{(m)}$  use (14);

//The blocking probabilities ;

$M_i^{(m)}$  using (10) and  $C_i^{(m)}$  using (11);

$M_{i,i+1}^{(m)}$  using (15) and  $C_{i,i+1}^{(m)}$  using using (16);

**end**

$m = m + 1$ ;

**until** *The steady-state probabilities probabilities at each queueing node converge ;*

**Algorithm 1:** Single-Node Decomposition Algorithm for a Queueing Network where the Bursts Span One or Two Links and a Large Number of Wavelengths

$$\begin{aligned} |\pi_i^{(m)} - \pi_i^{(m-1)}| &< \epsilon, & 1 \leq i \leq K \\ |\pi_{i,i+1}^{(m)} - \pi_{i,i+1}^{(m-1)}| &< \epsilon, & 0 \leq i \leq K-1, \end{aligned}$$

where  $\epsilon$  is a sufficiently small positive number. We note that the blocking probability of short bursts at link  $i$  should be equal to the blocking probability of long bursts at link  $i$ , i.e.,  $M_i = M_{i-1,i}$ . This is due to the full wavelength conversion assumption (see Section 2).

## 5 Example

To illustrate our algorithm let us take a simple but non-trivial example of an OBS path with  $K = 3$  links. The main arrivals to this OBS path are Poisson distributed and the mean rate for the short bursts is  $\lambda_1 = 1$  and for the long bursts is  $\lambda_{01} = 1$ . The cross arrivals are also Poisson-distributed and their means are  $\gamma_s = 1$  for the short bursts and  $\gamma_l = 1$  for the long. Each burst holds a wavelength on a link for an exponential time with an average  $1/\mu = 1$  before releasing the wavelength and acquiring a new wavelength on the next link.

We begin by constructing a queuing network model as explained in Section 3. For the initial guess of the steady state probability vectors at each queueing node we use (1) for a short node and (2) for a long node. The main and cross burst loss probabilities at a node are approximated by the steady state probabilities of the node having all of its  $W$  wavelengths busy.

Next, we proceed with the algorithm by taking into account the dependencies between the queueing nodes. For the iterative step  $m$  we show in detail how to obtain the blocking probabilities at short node 1 and long node 01. The same methodology is applied to the rest of the nodes:

- at node 1: The arrival rate  $\lambda_1$  is given. The steady state probabilities are

$$\begin{aligned} \pi_1^{(m)}(j) &= \pi_1^{(m)}(0) \frac{\lambda_1^j}{j! \mu^j} \prod_{m=0}^{j-1} Prob\{\text{link1 is not full} \mid n_1 = m\}, \quad 0 \leq j \leq W \\ &= \pi_1^{(m)}(0) \frac{\lambda_1^j}{j! \mu^j} \prod_{m=0}^{j-1} Prob\{n_{01} + n_{12} < (W - m) \mid n_1 = m\} \\ &= \pi_1^{(m)}(0) \frac{\lambda_1^j}{j! \mu^j} \prod_{m=0}^{j-1} P_1^1(m) \\ &= \pi_1^{(m)}(0) \frac{\lambda_1^j}{j! \mu^j} \prod_{m=0}^{j-1} \left[ \sum_{s=0}^{W-m} \pi_{01}^{(m-1)}(s) \sum_{t=0}^{W-m-s} \pi_{12}^{(m-1)}(t) \right]. \end{aligned}$$

The main burst blocking probability is

$$\begin{aligned} M_1^{(m)} &= \sum_{j=0}^W \pi_1^{(m)}(j) Prob\{\text{link 1 is full} \mid n_1 = j\}, \quad 0 \leq j \leq W \\ &= \sum_{j=0}^W \pi_1^{(m)}(j) Prob\{n_{01} + n_{12} \geq (W - j) \mid n_1 = j\} \\ &= \sum_{j=0}^W \pi_1^{(m)}(j) (1 - P_1^1(j)). \end{aligned}$$

There is no cross traffic at node 1 and thus  $C_1^{(m)} = 0$ .

- at node 01: The arrival rate  $\lambda_{01}$  is given. The steady state probabilities are

$$\begin{aligned}
\pi_{01}^{(m)}(j) &= \frac{\pi_{01}^{(m)}(0)}{j! \mu^j} \prod_{m=0}^{j-1} \lambda_{01} \text{Prob}\{\text{link 1 is full} \mid n_{01} = j\}, \quad 0 \leq j \leq W \\
&= \frac{\pi_{01}^{(m)}(0)}{j! \mu^j} \prod_{m=0}^{j-1} \lambda_{01} \text{Prob}\{n_1 + n_{12} < (W - m) \mid n_{01} = m\} \\
&= \frac{\pi_{01}^{(m)}(0)}{j! \mu^j} \prod_{m=0}^{j-1} \lambda_{01} P_1^{01}(m) \\
&= \frac{\pi_{01}^{(m)}(0)}{j! \mu^j} \prod_{m=0}^{j-1} \lambda_{01} \left[ \sum_{s=0}^{W-m} \pi_1^{(m)}(s) \sum_{t=0}^{W-m-s} \pi_{12}^{(m-1)}(t) \right].
\end{aligned}$$

Note that we use  $\pi_1^{(m)}$  since we have already calculated it in the previous step.

The main blocking probability is

$$\begin{aligned}
M_{01}^{(m)} &= \sum_{j=0}^W \pi_{01}^{(m)}(j) \text{Prob}\{\text{link 1 is full} \mid n_{01} = j\}, \quad 0 \leq j \leq W \\
&= \sum_{j=0}^W \pi_{01}^{(m)}(j) \text{Prob}\{n_1 + n_{12} \geq W - j \mid n_{01} = j\} \\
&= \sum_{j=0}^W \pi_{01}^{(m)}(j) (1 - P_1^{01}(j)).
\end{aligned}$$

There is no cross traffic at node 01 and thus  $C_{01}^{(m)} = 0$ .

When  $W = 2$  wavelengths per link, the single-node decomposition algorithm converges in seven iterations as shown in Table 1. Note that the analytical results are very close to those obtained through simulation.

## 6 Numerical Results

We verify our single-node decomposition algorithm by using simulation. The analytical algorithm was programmed in Matlab, whereas for the simulation we have developed a custom event-driven C++ simulator. For the simulation results, we include the 95% confidence intervals but they are hardly visible on the plots.

We have tested our algorithm extensively and we have observed that it always gives results close to the results obtained through the simulation. We present 15 plots for an OBS path with  $K=7$  links. We vary the number of wavelengths  $W = 50$  (Figure 6-13),  $W = 100$  (Figure 14-21) and  $W = 200$  (Figure 22-29). For each value of  $W$  we also vary the mixture of short and long bursts by changing the probability that

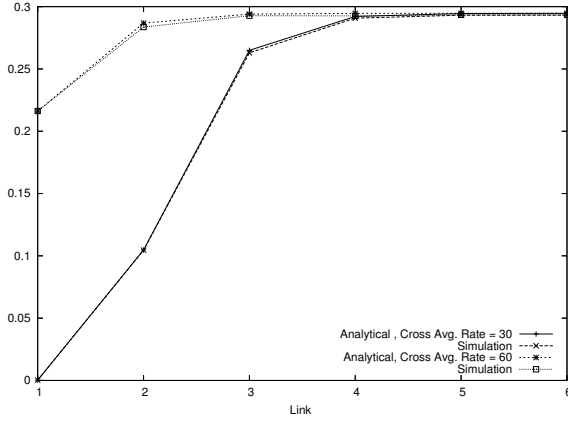


Figure 6: Short Burst Loss Probability,  $W=50$ ,  $K=7$ ,  $\gamma = 20$ ,  $P_{sh} = 1$

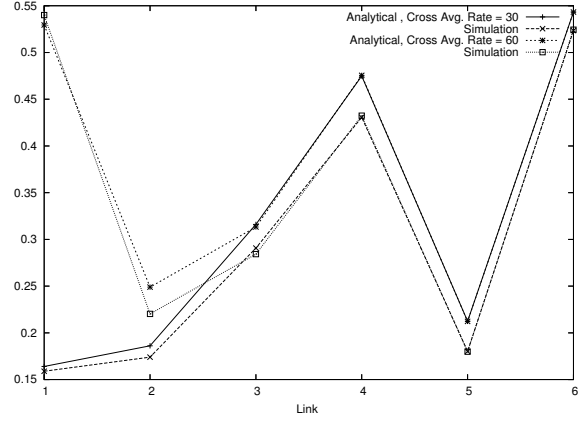


Figure 7: Long Burst Loss Probability,  $W=50$ ,  $K=7$ ,  $\gamma = 20$ ,  $P_{sh} = 0$

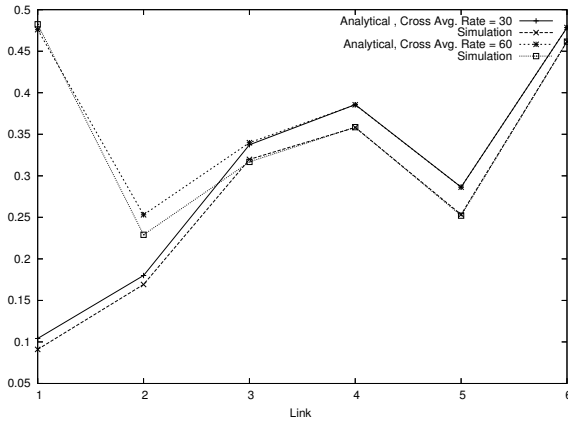


Figure 8: Short Burst Loss Probability,  $W=50$ ,  $K=7$ ,  $\gamma = 20$ ,  $P_{sh} = 0.25$

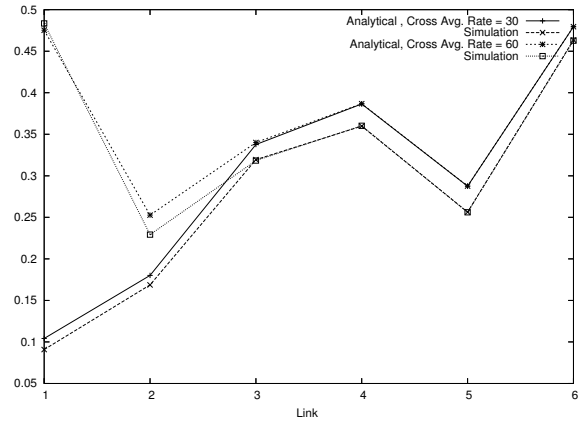


Figure 9: Long Burst Loss Probability,  $W=50$ ,  $K=7$ ,  $\gamma = 20$ ,  $P_{sh} = 0.25$

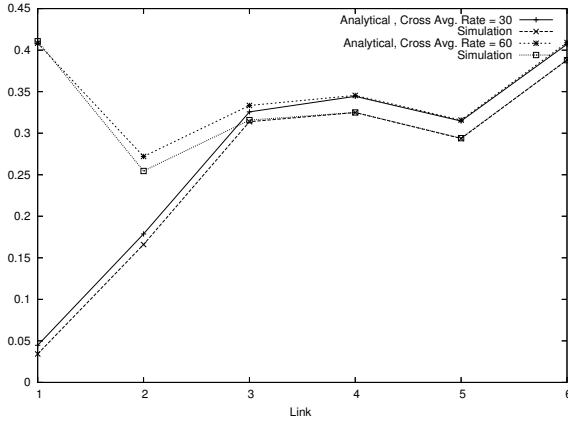


Figure 10: Short Burst Loss Probability,  $W=50$ ,  $K=7$ ,  $\gamma = 20$ ,  $P_{sh} = 0.5$

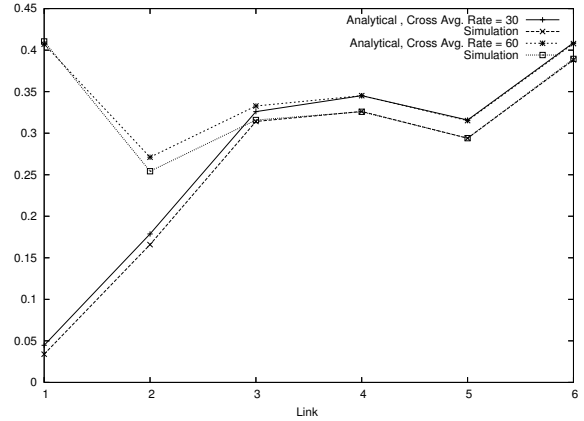


Figure 11: Long Burst Loss Probability,  $W=50$ ,  $K=7$ ,  $\gamma = 20$ ,  $P_{sh} = 0.5$

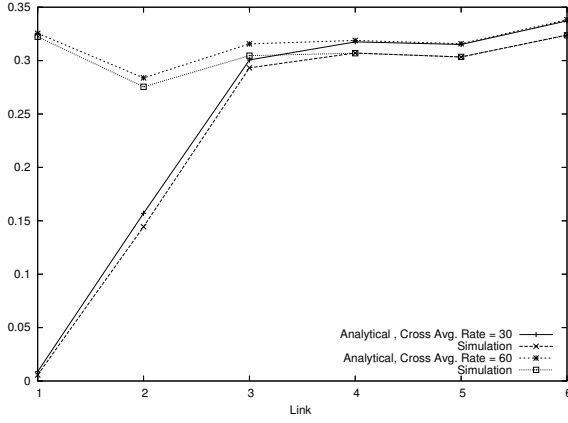


Figure 12: Short Burst Loss Probability,  $W=50$ ,  $K=7$ ,  $\gamma = 20$ ,  $P_{sh} = 0.75$

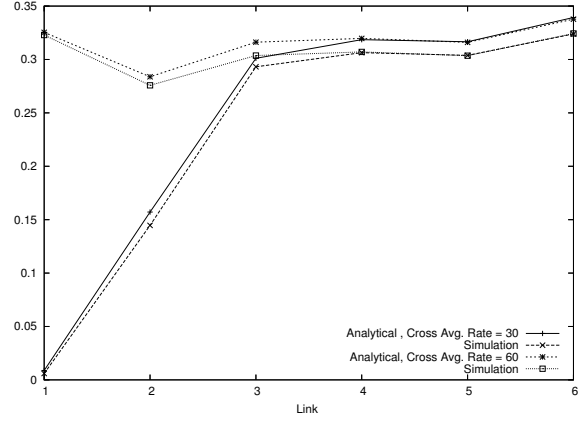


Figure 13: Long Burst Loss Probability,  $W=50$ ,  $K=7$ ,  $\gamma = 20$ ,  $P_{sh} = 0.75$

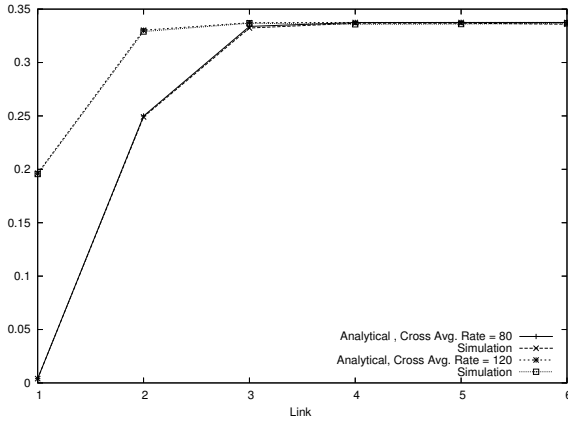


Figure 14: Short Burst Loss Probability,  $W=100$ ,  $K=7$ ,  $\gamma = 50$ ,  $P_{sh} = 1$

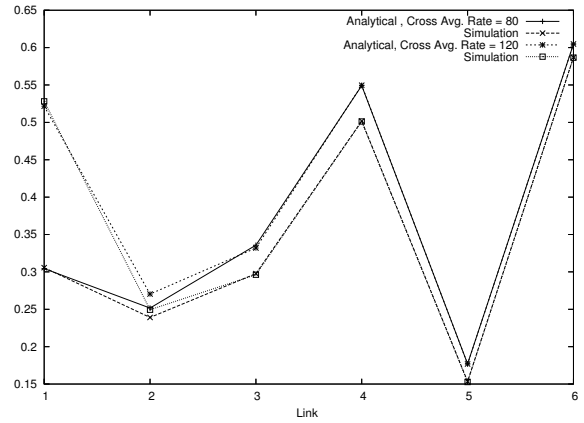


Figure 15: Long Burst Loss Probability,  $W=100$ ,  $K=7$ ,  $\gamma = 50$ ,  $P_{sh} = 0$

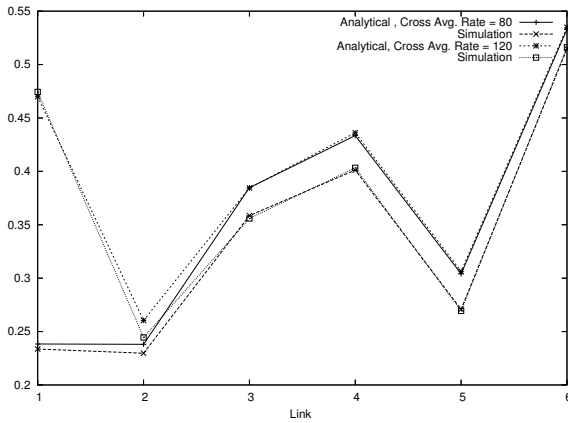


Figure 16: Short Burst Loss Probability,  $W=100$ ,  $K=7$ ,  $\gamma = 50$ ,  $P_{sh} = 0.25$

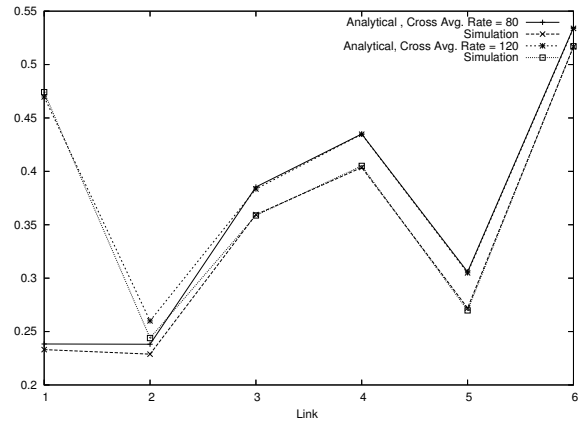


Figure 17: Long Burst Loss Probability,  $W=100$ ,  $K=7$ ,  $\gamma = 50$ ,  $P_{sh} = 0.25$

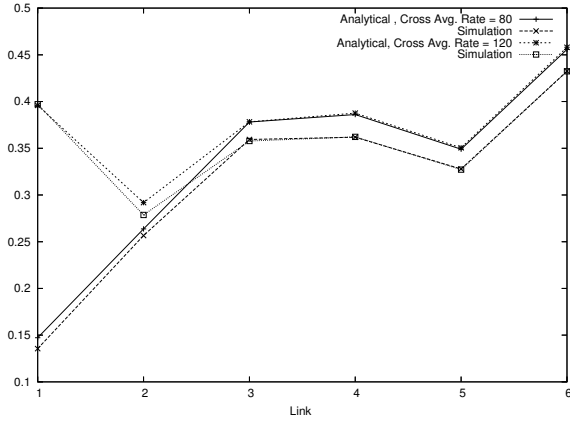


Figure 18: Short Burst Loss Probability,  $W=100$ ,  $K=7$ ,  $\gamma = 50$ ,  $P_{sh} = 0.5$

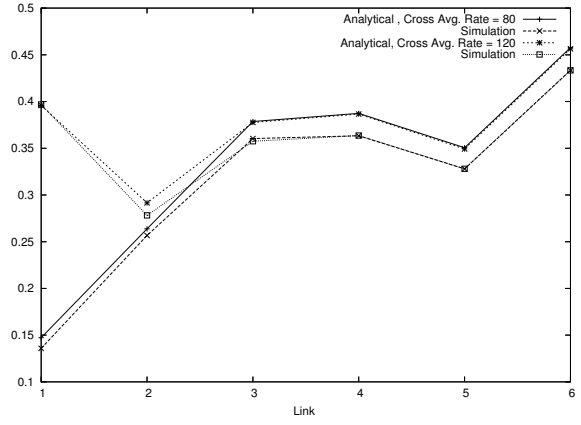


Figure 19: Long Burst Loss Probability,  $W=100$ ,  $K=7$ ,  $\gamma = 50$ ,  $P_{sh} = 0.5$

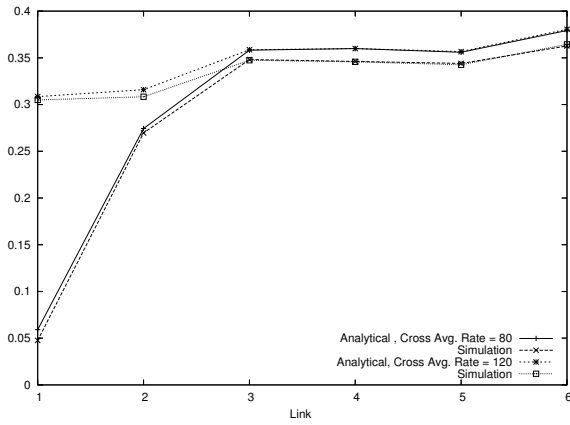


Figure 20: Short Burst Loss Probability,  $W=100$ ,  $K=7$ ,  $\gamma = 50$ ,  $P_{sh} = 0.75$

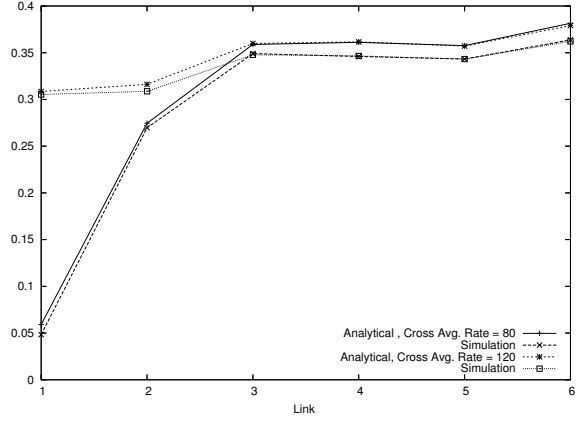


Figure 21: Long Burst Loss Probability,  $W=100$ ,  $K=7$ ,  $\gamma = 50$ ,  $P_{sh} = 0.75$

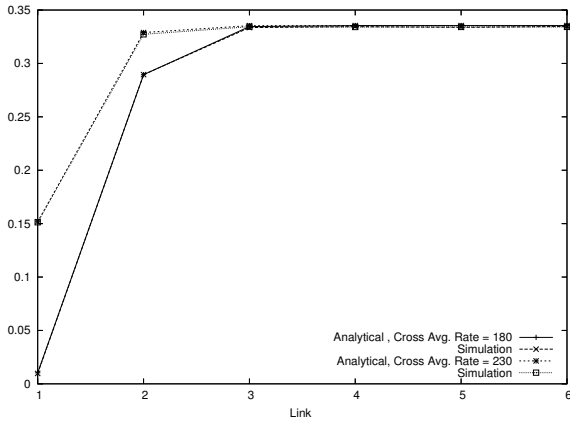


Figure 22: Short Burst Loss Probability,  $W=200$ ,  $K=7$ ,  $\gamma = 100$ ,  $P_{sh} = 1$

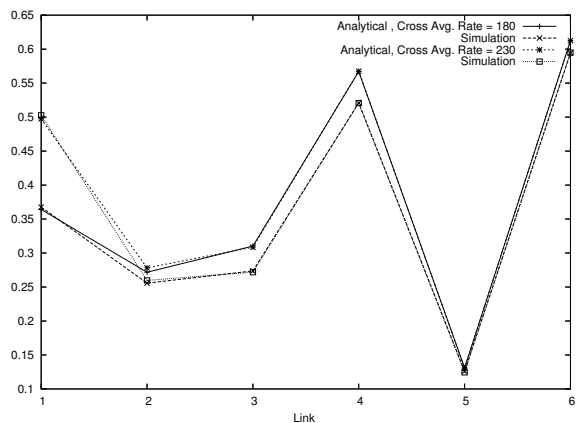


Figure 23: Long Burst Loss Probability,  $W=200$ ,  $K=7$ ,  $\gamma = 100$ ,  $P_{sh} = 0$

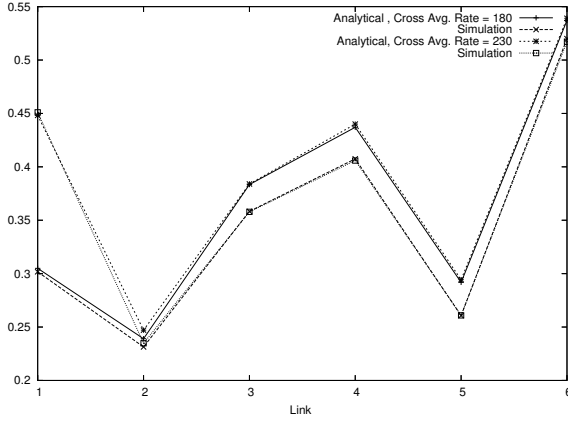


Figure 24: Short Burst Loss Probability,  $W=200$ ,  $K=7$ ,  $\gamma = 100$ ,  $P_{sh} = 0.25$

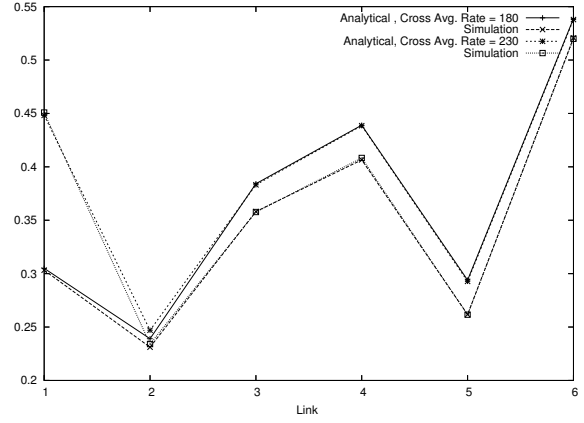


Figure 25: Long Burst Loss Probability,  $W=200$ ,  $K=7$ ,  $\gamma = 100$ ,  $P_{sh} = 0.25$

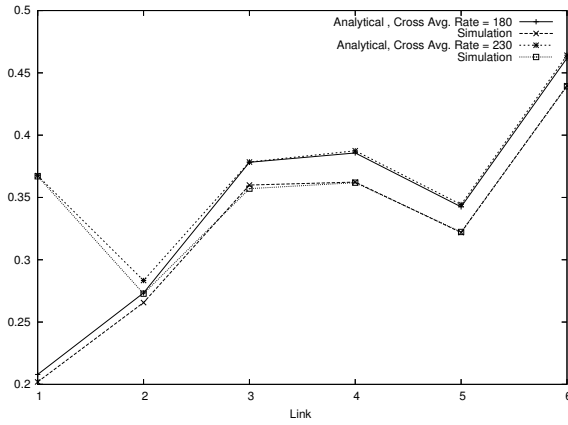


Figure 26: Short Burst Loss Probability,  $W=200$ ,  $K=7$ ,  $\gamma = 100$ ,  $P_{sh} = 0.5$

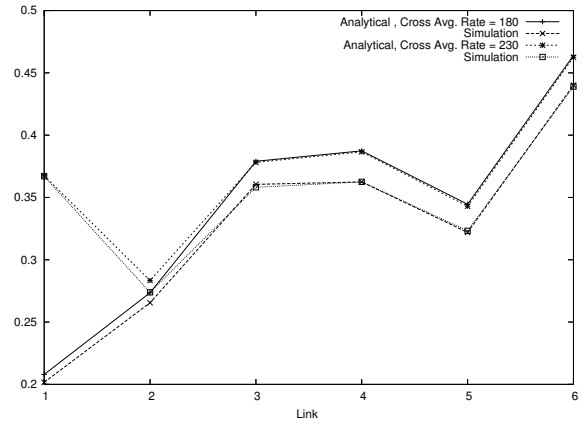


Figure 27: Long Burst Loss Probability,  $W=200$ ,  $K=7$ ,  $\gamma = 100$ ,  $P_{sh} = 0.5$

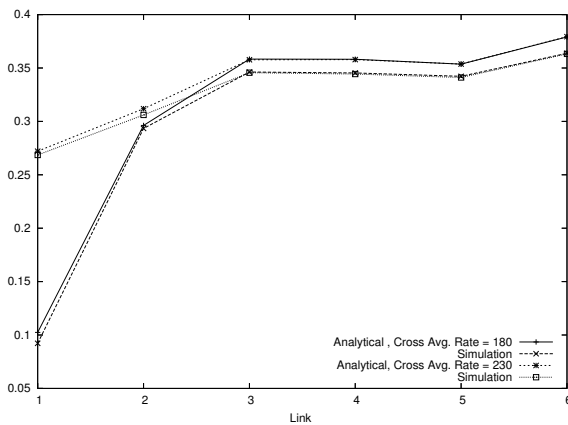


Figure 28: Short Burst Loss Probability,  $W=200$ ,  $K=7$ ,  $\gamma = 100$ ,  $P_{sh} = 0.75$

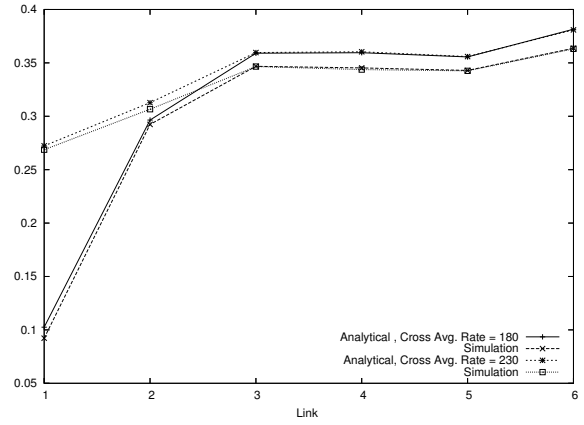


Figure 29: Long Burst Loss Probability,  $W=200$ ,  $K=7$ ,  $\gamma = 100$ ,  $P_{sh} = 0.75$

Iteration	Short Burst Loss			Long Burst Loss		
	Link 1	Link 2	Link 3	Link 1	Link 2	Link 3
1	0.56161	0.51782	0.32564	0.67292	0.68504	0.50320
2	0.40984	0.46150	0.41016	0.34558	0.40597	0.41017
3	0.45360	0.47685	0.39317	0.47105	0.49268	0.39574
4	0.43300	0.47968	0.39794	0.42452	0.47652	0.39807
5	0.43789	0.47933	0.39670	0.43988	0.48021	0.39671
6	0.43626	0.47953	0.39705	0.43559	0.47928	0.39705
7	0.43668	0.47947	0.39695	0.4368	0.47954	0.39695
Simulation	0.43934	0.48751	0.38038	0.43912	0.48733	0.37955

Table 1: Burst Loss Probabilities for an OBS Path with  $K = 3$  Links,  $W = 2$  Wavelengths, Main Mean traffic rates  $\lambda_1 = 1$  and  $\lambda_{01} = 1$ , Cross Mean traffic rates  $\gamma_s = 1$  and  $\gamma_l = 1$

$P_{sh}$	0	0.25	0.5	0.75	1
$P_{lng}$	1	0.75	0.5	0.25	0

Table 2: Probability Mixtures of Short and Long bursts

an arrival is a short burst  $P_{sh}$  or long burst  $P_{lng} = (1 - P_{sh})$ . This mixture is set for both the main and cross traffic bursts and we consider the five cases from Table 2.

On each plot we vary the load of the main burst traffic by varying the mean arrival rate, i.e., from low load to high load. We observe a filtering phenomenon. In other words, the input main load only matters for the first few links of the path. By links 4 through 6 all the high input load is filtered out and thus the blocking probability converges. In Table 3, we show the relative % error for each of the considered cases. We observe that the relative error of our algorithm stays below 10%. The highest error is in the case where  $P_{sh} = 1$  and  $W = 50$ . The reason is that in this case the value of the burst loss probability at link 1 is very small, i.e.,  $2.449E - 4$  in the simulation and  $2.2E - 4$  when analytically computed. Note that in the presented plots, our analytical solution gives an upper bound for the blocking probabilities. In Table 4, we show the number of iterations for each case. As the number of wavelengths increases so does the number of iterations. Note that if only short bursts are present, i.e.,  $P_{sh} = 1$ , there is no simultaneous link possession and the algorithm goes through only one iteration.

W	50					100					200				
$P_{sh}$	0	0.25	0.5	0.75	1	0	0.25	0.5	0.75	1	0	0.25	0.5	0.75	1
Short	-	7.69	7.69	8.81	110.20	-	8.13	8.58	4.57	1.14	-	8.41	7.07	4.45	5.78
Long	9.99	7.42	7.77	8.66	-	9.68	7.79	8.40	4.88	-	8.98	7.99	7.02	4.91	-

Table 3: Maximum Relative Errors

W	50					100					200				
$P_{sh}$	0	0.25	0.5	0.75	1	0	0.25	0.5	0.75	1	0	0.25	0.5	0.75	1
Low Load	12	19	24	21	1	18	30	42	38	1	31	45	66	62	1
High Load	13	14	15	14	1	19	24	33	21	1	32	44	45	39	1

Table 4: Number of Iterations

## 7 Conclusions

In this paper, we developed a queueing network model for an OBS path with dynamic simultaneous link possession and large number of wavelength per link. We assumed that the bursts, having variable size, arrive according to a Poisson process. We developed a single-node decomposition algorithm, suitable for networks with large number of wavelength per link, to approximate for the burst loss probabilities and tested its accuracy. Comparison against simulation results suggests that our algorithm has a good accuracy. We also note, that for the presented numerical results, our algorithm was time effective. The simulation time was between thirty minutes to one hour, while the time needed to obtain the results using the single-node decomposition algorithm was always less than a few minutes.

## References

- [1] J. Wei and R. McFarland. Just-in-time signaling for WDM optical burst switching networks. *Journal of Lightwave Technology*, 18(12):2019–2037, December 2000.
- [2] T. Battestilli and H. Perros. An introduction to optical burst switching. *IEEE Communications Magazine*, 41(8):S10–S15, August 2003.
- [3] C. Qiao and M. Yoo. "Optical burst switching (OBS)- a new paradigm for an Optical Internet". *Journal of High Speed Networks*, 8(1):69–84, January 1999.
- [4] Yijun Xiong, M M. Vandenhouste, and H. Cankaya. Control architecture in optical burst-switched WDM networks. *IEEE Journal on Selected Areas in Communications*, 18(10):1838–1851, October 2000.
- [5] K. Dolzer, C. Gauger, J. Spath, and S. Bodamer. Evaluation of reservation mechanisms for optical burst switching. *AEU International Journal of Electronics and Communications*, 55(1), 2001. January.
- [6] M. Yoo, C. Qiao, and S. Dixit. QoS performance of optical burst switching in IP-over-WDM networks selected areas in communications. *IEEE Journal on Areas in Communications*, 18(10):2062–2071, 2000. October.
- [7] Hai Le Vu and M. Zukerman. Blocking probability for priority classes in optical burst switching networks. *IEEE Communications Letters*, 6(5), May 2002.

- [8] Xiaomin Lu and B.L. Mark. A new performance model of optical burst switching with fiber delay lines. In *Proceedings of the IEEE International Conference on Communications, 2003. ICC '03.*, volume 2, pages 1365–1369, May 2003.
- [9] Ching-Fang Hsu, Te-Lung Liu, and Nen-Fu Huang. On the deflection routing in QoS supported optical burst-switched networks. *IEEE International Conference on Communications*, 5:2786–2790, 2002.
- [10] Yang Chen, Hongyi Wu, Dahai Xu, and Chunming Qiao. Performance analysis of optical burst switched node with deflection routing. In *Proceedings of the IEEE International Conference on Communications, 2003. ICC '03.*, volume 2, pages 1355–1359, May 2003.
- [11] K. Dolzer, C. Gauger, J. Spath, and S. Bodamer. Evaluation of reservation mechanisms for optical burst switching. *AEU International Journal of Electronics and Communications*, 55(1), 2001. January.
- [12] N. Barakat and E. H. Sargent. Analytical modeling of offset-induced priority in multiclass obs networks. *IEEE Transactions on Communications*, 53(8):1343–1352, 2005.
- [13] M. Duser and P. Bayvel. Analysis of a dynamically wavelength-routed optical burst switched network architecture. *IEEE Journal of Lightwave Technology*, 20(4):574–585, 2002.
- [14] Z. Rosberg, Hai Le Vu, M. Zukerman, and J. White. Performance analyses of optical burst-switching networks. *IEEE Journal on Selected Areas in Communications*, 21(7), Sept. 2003.
- [15] Andrew Zalesky, Hai Le Vu, Zvi Rosberg, Eric Wong, and Moshe Zukerman. Modeling and performance evaluation of optical burst switched networks with deflection routing and wavelength reservation. In *Proceedings of INFOCOM 2004*, Hong Kong, March 2004.
- [16] Leonard Kleinrock. *Queueing Systems Volume 1:Theory*. John Wiley and Sons, Inc., 1975.